

ADVANCED OPTICAL ROTOR BLADE DEFORMATION MEASUREMENTS ON A FLYING HELICOPTER

Fritz Boden¹, Anwar Torres¹, Christoph Maucher²

¹German Aerospace Center (DLR), Göttingen

²Eurocopter Deutschland GmbH; Ottobrunn

Abstract

The performance of a helicopter mainly depends on the design of the main rotor. They have to endure strong centrifugal and bending forces and should be able to transmit these loads to the rotor hub and therefore to the airframe. To design rotor blades which could fulfil these requirements, the loads occurring under flight conditions and the resultant behaviour of the rotor blades (flapping, lead-lag bending and twisting motion) have to be known. The in-flight investigation of the deformation of the fast spinning rotor is a demanding task. It is evident, that conventional methods such as strain gauges and accelerometers are difficult to use because of problems with their installation, wiring, the data transmission, and the balancing of the rotor. Additionally, such sensors provide data only at the location where they have been installed. Consequently, a non-intrusive and planar measurement of the rotor blade deformation in flight is of high interest.

This need for advanced, non-intrusive e.g. optical measurement techniques has been identified. Within the EC-funded specific targeted research project "AIM – Advanced In-flight Measurement Techniques" DLR and Eurocopter are applying the Quantitative Video Technique (QVT) together with the Image Pattern Correlation Technique (IPCT) to obtain the in-flight deformation of the main rotor blades of an EC-135. These advanced measurement techniques deliver 3D shape and deformation results by using stereoscopic camera pictures of the investigated objects, in this case, the EC-135 main rotor blades.

To check the usability of the QVT and the accuracy of the IPCT for industrial in-flight measurements, a test with an instrumented rotor blade has been performed. The present paper will give a short introduction to the challenging task and some basics of the used measurement techniques. The measuring system will be described and the performed tests will be presented. To conclude, some example results and a short outlook concerning future activities will be given.

1. INTRODUCTION

The rotor blades of a helicopter are heavily loaded due to strong centrifugal forces and periodically changing lift and moment distribution. Especially in fast forward flight of the helicopter the rotor blade passes from transonic flow at the advancing side to dynamic stall effects on the retreating side during each revolution. The knowledge about varying loads on the blades is required for an optimal design of the rotor. Usually strain gauges and accelerometers are used for flight tests to measure the deformation and movement of the rotorcraft structures. These sensors are highly sophisticated and give data of high accuracy within a short time. But they are able to deliver these data only at the location where they are positioned. The needed wiring and the big effort for installing the sensors in a way that they don't affect the aerodynamic and dynamic behaviour are also a drawback. Especially the installation in the rotary frame leads to strong limitations concerning the number of sensors due to the limited achievable data transmission and constraints for additional weight.

During the last years optical measurement techniques, which have the potential to replace strain gauges and accelerometers at several points, had been developed to measure model position and deformation of model structure in wind tunnels [1], [2], [3].

Within the AIM (Advanced In-flight Measurement techniques) project [4] various advanced non-intrusive measurement techniques are introduced for usage in flight testing of fixed and rotary wing aircraft. The novel techniques are considered as important for supporting future certification and in-flight research by taking advantage of these technique's efficiency, cost effectiveness, enhanced accuracy and capabilities.

One of these advanced optical measurement techniques is the Image Pattern Correlation Technique (IPCT) [3], which is applied by DLR and Eurocopter to measure the deformation of the main rotor blades of a Eurocopter EC-135 in combination with the Quantitative Video Technique (QVT).

2. THE TASK

For the design of a helicopter rotor blade, it is crucial to predict the dynamic behaviour and occurring forces and moments. For the validation of prediction tools, reliable flight test data are required. Furthermore, flight test measurements are necessary for the calculation of fatigue loads.

In forward flight, the asymmetric flow conditions of the rotor lead to periodically varying flow velocities and angle of attacks on the revolving blade. The alternating distribution of moments and forces excite blade oscillation in lead-lag, flapping and torsion with the rotational frequency or its higher harmonics. The highest blade loads occur in highly loaded flight conditions, especially turns or manoeuvre flight.

Today, strain gauges are applied to a helicopter rotor blade to perform measurements in flight test. Locally, they allow a precise strain measurement for the complete rotor revolution. In order to get a complete picture of the occurring blade loads, many strain gauges are necessary. Therefore, the instrumentation of the rotor blade implies a high effort. Furthermore, wiring can imply difficulties due to its weight and its perturbation of the aerodynamic shape.

An optical measurement technique may overcome some of the limitations of strain gauges. A precise measurement of the deformation of the complete surface of the rotor blade allows to locate high strains and to identify more oscillatory modes. Furthermore, the exact blade position can be identified optically.

3. THE MEASUREMENT TECHNIQUE

To measure the rotor blade deformation optically, two methods had been applied – the Image Pattern Correlation Technique (IPCT) and the Quantitative Video Technique (QVT). Both are described in the following subchapters.

3.1. The IPCT

The IPCT is an optical, non-intrusive measurement technique, based on photogrammetry in combination

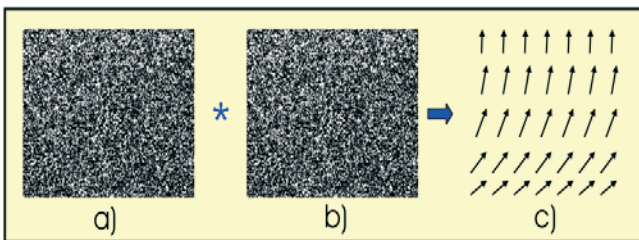


Figure 1: Principle of IPCT (a - reference image, b - deformed image, c - displacement vectors).

with modern cross correlation algorithms developed for Particle Image Velocimetry (PIV). The simplest IPCT setup consists of one monochrome camera observing an object covered with a random dot pattern. After a reference image of the investigated object has been acquired (Figure 1a) the object will be set into a load condition which causes its deformation. The second image (Figure 1b) will be recorded under such deformed state. The image of the deformed object will be cross-correlated with the reference image. A 2D displacement vector field (Figure 1c) will be obtained as result.

Using image pairs of the randomly patterned object acquired by a stereoscopic camera system, its 3D position and shape can be obtained. Figure 2 schematically shows the functionality of stereoscopic IPCT. During the first step the investigated surface $H(X;Y)$ with the random dot pattern is recorded by two cameras (camera 1 and camera 2). Both cameras are looking at the same field of view, but under different viewing angles. A cross correlation algorithm identifies the coordinates of areas with similar dot patterns in the images of camera 1 (coordinates x_1, y_1) and camera 2 (coordinates x_2, y_2).

With known intrinsic parameters (e.g. focal length, distortion, principal point) and extrinsic parameters (position and orientation) of both cameras, the 3D coordinates of the recognized areas with the same dot pattern are determined by means of central projection and triangulation.

The application of this algorithm to all areas in the images depicting the same dot pattern regions on the surface finally yields to a highly accurate reconstruction of the complete 3D surface.

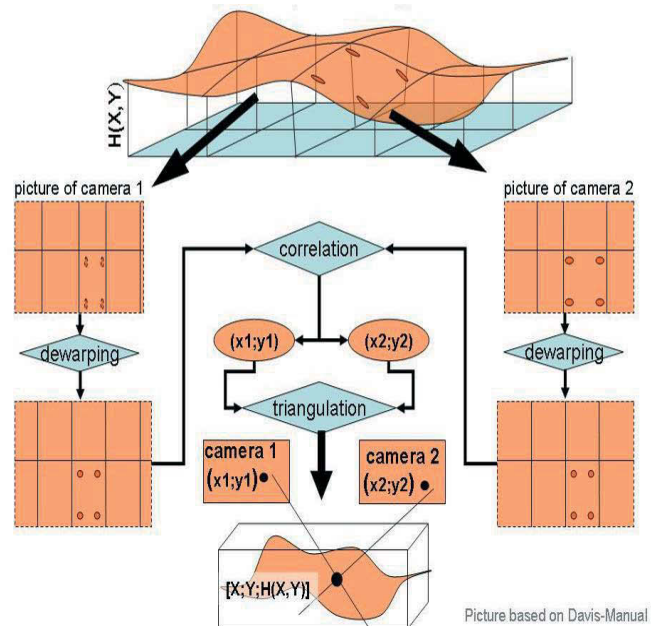


Figure 2: Procedure of stereoscopic IPCT for 3D measurement.

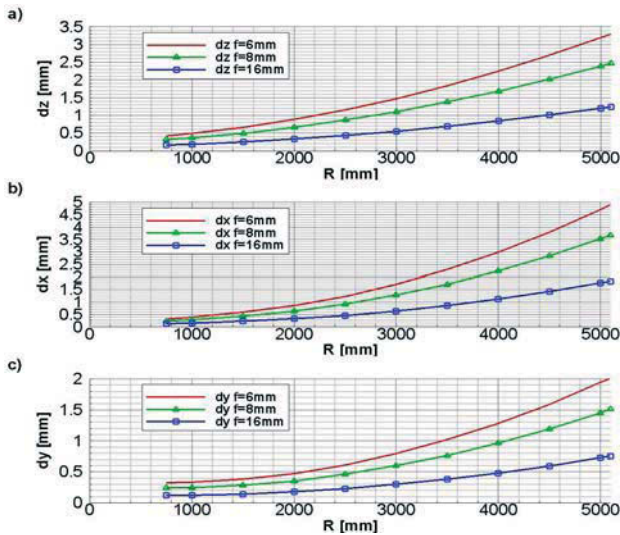


Figure 3: Theoretical accuracy of an IPCT setup (a - dz perpendicular to the blade; b - dx spanwise; c - dy chordwise).

By comparing the measured 3D surface under a well known reference state (e.g. a wing of an aircraft standing on ground) to the surface under load conditions (e.g. the wing deformed during flight), the displacement vectors and thus the deformation can be deduced with a high accuracy. If the material characteristics of the observed object are known the local stress can be easily calculated.

The advantage of the stereoscopic setup is that the location of the surface under investigation can be measured and that motion in all directions can be determined. The main advantage of IPCT is the simplicity of its basic experimental setup: In principle a foil furnished with a random dot pattern and two standard CCD cameras are sufficient to determine the shape of the investigated surface with a high accuracy. Theoretically the accuracy of IPCT is in the order of 0.01 % of the observed area (e.g. 0.1 mm on 1 m), depending on the observation angle, the pixel resolution of the camera and the used optics. According to [7], the diagram in Figure 3 gives some estimation of the accuracy of the IPCT setup intended for the rotor blade investigations. The coordinate R stands for the radius of the observed chord on the rotor blade, while dx , dy and dz give the error (respectively the accuracy) in spanwise, chordwise and perpendicular direction of the blade. For the calculation, the JAI CV A1 camera is located at $R = 750$ mm and 1400 mm below the rotor blade. The dependency on the distance is clearly visible as the error increases from the root to the tip of the blade. This is due to the decreasing observation angle which causes an increase of the length in spanwise direction in mm imaged on an area of 1 pixel on the camera chip. It can also be seen, that the accuracy is depending on the focal length f of the camera. It is obvious that with a higher focal length (i.e. magnification) the imaging becomes more

detailed.

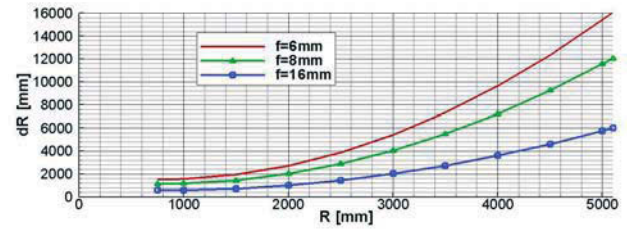


Figure 4: Spanwise size of the region measured on the blade.

The drawback of a higher magnification is the reduction of the measurement area. Figure 4 shows the dependency of the measurement area's spanwise size to the rotor radius R and the focal length f . To have a good compromise between accuracy and size of the measurement area and to use the advantage of IPCT to get results over a big surface area, the focal length $f = 8$ mm and the measurement region from $R = 1000$ mm to $R = 3000$ mm was chosen for the presented test on the EC 135. The accuracy for displacements of the blade over 2 m span therefore is expected to be 0.5 to 1 mm for dz , 0.5 to 1.2 mm for dx and 0.3 to 0.6 mm for dy .

3.2. The QVT

The qualitative visualization of flows and moving objects has been improved considerably by the development of CCD sensors with high temporal and spatial resolution. Due to the processing power of modern computers the image data can also be rapidly analysed to yield quantitative information about location, geometry, intensity etc. and the structure of such objects. At DLR a special multi-camera video system – the High-Speed Video-Stroboscope [6] - has been developed for various applications of quantitative visualization. The cameras of this system work in non-standard video mode, i.e. they can be freely programmable shuttered and triggered and they can be synchronized to external events. In the case of periodic events, the image acquisition can be performed at freely selectable phase angles (i.e. positions of the rotating object); even in cases when the rotational speed of the object is slowly varying.

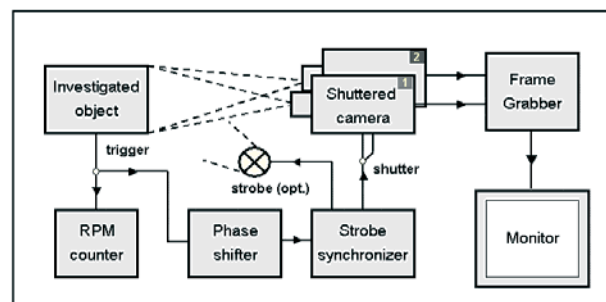


Figure 5: Block circuit of the video stroboscope.

The IPCT images of the helicopter main rotor blade have been acquired by means of QVT with the existing High-Speed Video-Stroboscope. It can control simultaneously up to four cameras of CV-M10, CV-A1 or CV-A2 type manufactured by JAI company.

The principle of this apparatus is shown in Figure 5. The shutter of the electronic camera(s) is controlled by the trigger signal received from the rotor. The position of the rotor blade on the image can be varied by means of the phase shift between the trigger pulses input from the rotor and the camera shutter control pulses.

For static deformation or for very slow object movement any standard camera can be applied. Special requirements appear for imaging of fast moving objects, like the main rotor blade of a helicopter observed from the fixed frame. In this case the shutter of the camera must be precisely synchronized with the movement of the object and the image integration time (comparable with the exposure time) must be short enough to prevent motion smear (Figure 6).

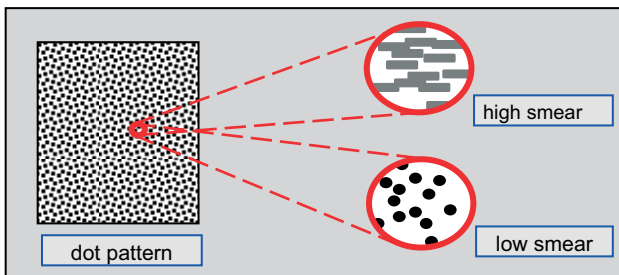


Figure 6: The dot smear caused by the object motion.

To ensure a sufficient exposure while having very short exposure times, high illumination intensity must be provided. Therefore a fast triggerable strobe light with sufficient power has to be applied.

3.3. The setup for the rotor blade measurements

As mentioned above a QVT recording system is needed to measure the main rotor blade deformation by means of IPCT. This system should consist of at least two cameras, one strobe light, a triggering device and of course a control and recording system. For the test within AIM it was decided to have everything in the fixed frame to ease the installation on the helicopter. This gives just the ability to record a cut-out of the rotor disc, but is sufficient to show the applicability of the method.

The designed camera system is depicted in Figure 7. It consists of two JAI CV-A1 cameras affixed on a very rigid basic support mounted at the helicopters' fix points for an external hoist system.



Figure 7: The experimental set-up installed at the helicopter (1, 2 – mountings; 3 – support; 4, 5 – cameras; 6 – strobe light; 7 – laser sensor).

To record without any jitter and with a very short shutter time the cameras had been upgraded with a new timing generator. The modified JAI CV-A1 camera has a resolution of $1380 \times 1035 \text{ pixel}^2$ and a minimal triggered shutter time of $2 \mu\text{s}$ ($= 1/500000 \text{ s}$) without any jitter.

To illuminate the observed area an Alluris SMS 300 digital high-end stroboscope is used. This fast triggerable strobe light can be powered with 28 V. Without external power it runs for around one hour on battery.

For the triggering of the system to the rotor, a laser sensor pointing to a reflector on the rotor hub is used. This gives one TTL-pulse per revolution for the system to adjust the instant of time for the recording of the images.

The investigated rotor blade was painted with a suitable speckle pattern to enable the IPCT processing of the images. Parts of it can be seen in Figure 8. The dot size of this pattern was chosen that way that one dot equals around 1.2 pixels. The speckle pattern on the rotor blade had been applied to the rotor blade with a spray gun operating at low pressure and thus producing bigger droplets. In addition to the small dots for IPCT big markers (big white dots with a black circle around) are painted on the rotor blade. These are used to identify the solid body movement of the blade and to separate it from the local deformation.

Furthermore the rotor blade is equipped with some strain gauges to compare the IPCT to a classical proven measurement technique.



Figure 8: Rotor blade with speckle pattern and markers.

4. WHIRLTOWER TEST (WTT)

To check the functioning of the measurement setup a first test had been performed during the tracking and balancing of the instrumented and speckled rotor blade on the Eurocopter Whirl tower in Donauwörth. Below this test is described.

4.1. Setup

For the whirl tower test (WTT) in Donauwörth, the cameras, the triggering device and the strobe light had been arranged in the same way like for the helicopter flight test (see Figure 9 and Figure 10). The High-Speed Video-Stroboscope, which was used to control the cameras and the strobe light, was placed in the whirl tower and controlled via Ethernet connection using a laptop with remote desktop in the control stand around 40 m away. In the control stand also the data acquisition for the strain gauges and the control of the whirl tower were located. To check the triggering stability of the reflector based method, the triggering was performed by the laser sensor and by the one per revolution pulse of the whirl tower itself.

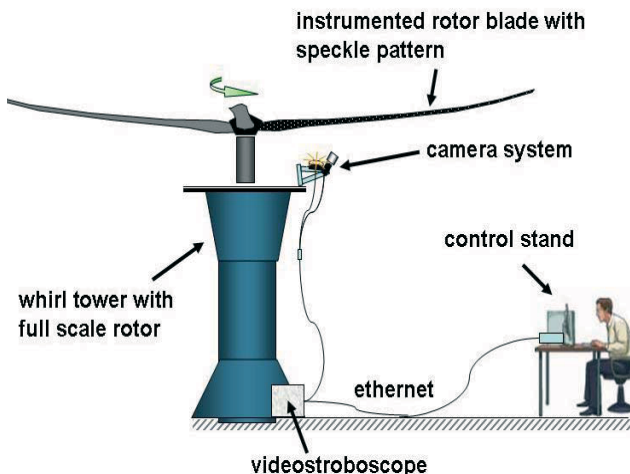


Figure 9: Scheme of setup for the whirl tower test (WTT).

To have similar boundary conditions like on the helicopter, the camera system had been placed on the platform of the whirl tower. The distance between cameras and rotor blade was around 1300 mm. The focal length of the cameras had been chosen to $f = 8$ mm and thus the observed blade area was around 1300 mm x 300 mm.

After finishing the installation and adjusting the field of view, the camera system had been calibrated by placing a plate with a regular dot grid under different orientations in front of the cameras.

During the test different collective pitch angles going from -3° to 14° had been driven to get different rotor loadings to be measured with both, strain gauges and IPCT.



Figure 10: Camera system on the whirl tower (1 - support; 2,3 - cameras; 4 - strobe light; 5 - laser sensor; 6 - whirl tower platform).

4.2. Results

A sample of the recorded images is shown in Figure 11. The rotor blade is in the right position for every image, which indicates triggering without jitter. The images are well exposed and no motion blur occurs. The pattern and the markers have a good contrast and sharpness which is very important for the IPCT post processing. The shutter speed for this recording was $1/120000$ s ($8.3 \mu\text{s}$) due to the high rotor speed and the viewing direction to the bright sky. It can be seen that for these conditions the use of a strobe light was mandatory. The spot characteristic of the strobe light is visible on these recordings and causes some higher brightness in the centre of the pictures and less on the border. This should be improved in the future to get a more homogenous illumination.

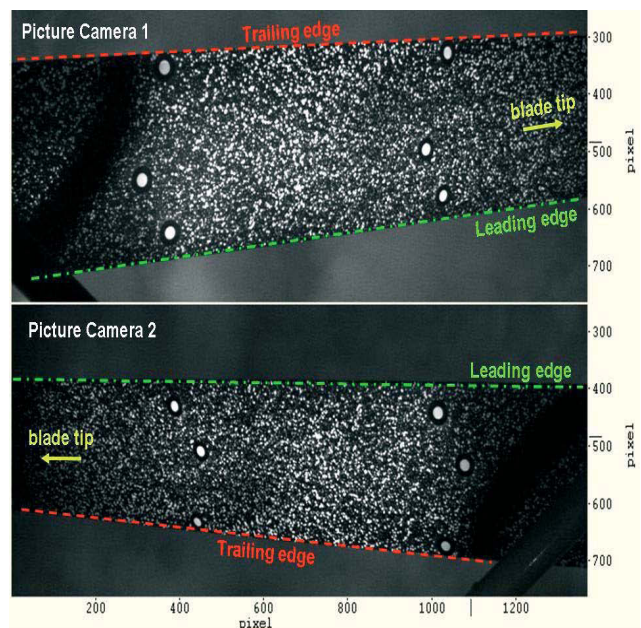


Figure 11: Sample of recorded images.

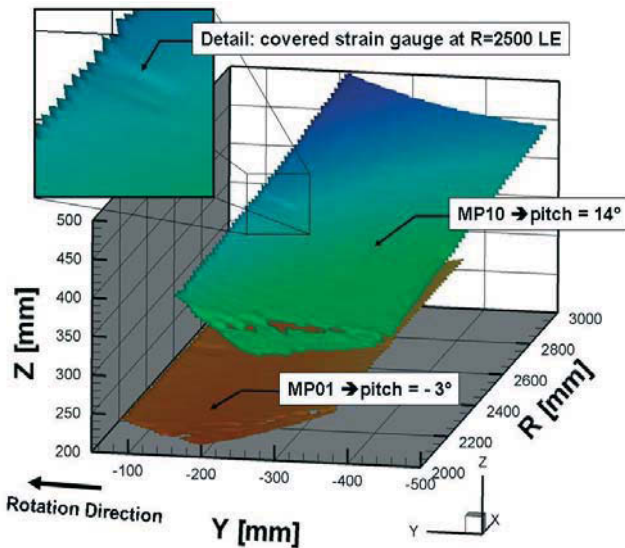


Figure 12: 3D-surface calculated from the images of different measurement points.

Nevertheless, the image data can be processed with the IPCT. Figure 12 shows some samples of the 3D-surfaces calculated from the images recorded at different pitch angles. It can be seen, that the observed cut out of the lower side of the rotor blade is reconstructed very well. Even details, like the raise due to the covered strain gauge close to the leading edge (LE) at R = 2500 mm, can be reproduced.

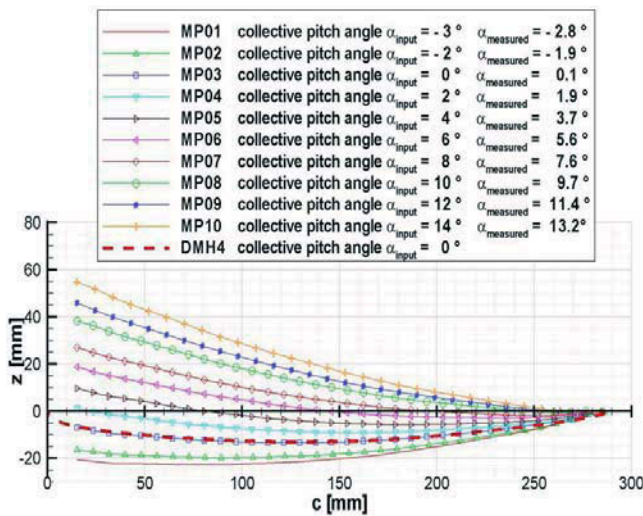


Figure 13: Measured profiles of the blades' lower surface extracted at R = 2300 mm and measured pitch angles against set collective pitch angles.

The combination of the IPCT with a stereoscopic marker detection algorithm allows the determination of the solid body movement of the observed cut out of the blade separated from the surface deformation. The movement of the rotor blade, especially the heave and the change of the angle of attack, can be seen in Figure 12.

Figure 13 shows chordwise profile lines extracted

from the calculated surfaces for the different measurement points at R = 2300 mm. The blades' local geometric angle of attack, which differs from the pitch angle given at the rotor hub, can be determined from these profiles. In Figure 13 the original rotor blade profile is included too. This allows a comparison between the original profile (the red dashed line) and the profile extracted from the IPCT – data, which fits very well with the measured profile at 0° pitch angle.

Triggering of the recording system by the laser sensor pointing to a reflector on the rotor blade produces images with the rotor blade in the same position every time. This makes recording easier but eliminates rotor blade movements in rotational direction. It could also cause a dependency of the triggering to the blades' pitch angle, which may create a shift in the blade position between different angles of attack. A triggering with the laser sensor pointing on a reflector on the rotor hub is thus to prefer.

In Figure 14 a sequence of recorded pictures is shown, which had been recorded by triggering to the rotor hub. The lead-lag and the oscillation of the blade in this direction can be seen clearly. The red lines and the six red circles in the frame with the label t_1 identify the start position of the blade which is compared to the following positions of the blade in the other frames representing different instants of time of the same measurement series. From t_1 to t_2 the blade moves towards the leading edge. At t_3 the blade has its maximum shift towards the leading edge and moves back towards the trailing edge for t_4 . After t_4 it reaches its start position like in t_1 and the oscillation starts again. The part of the whirl tower balustrade seen in the left lower image corner proves, that the movement is done by the rotor blade and is not caused by a movement of the cameras.

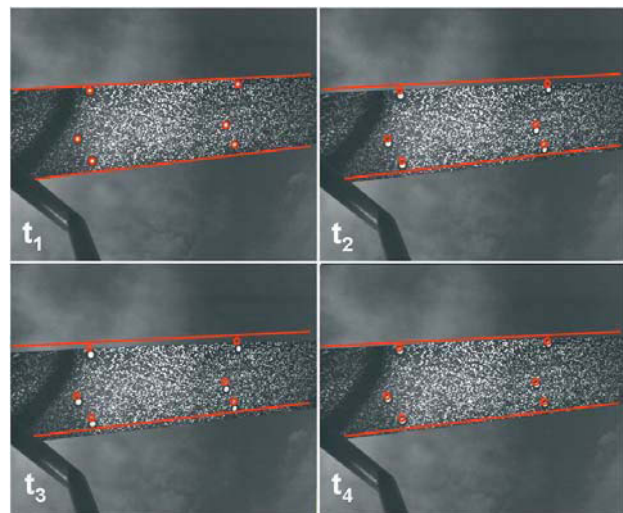


Figure 14: Sequence of recorded images for one pitch setting showing the lead-lag movement of the blade.

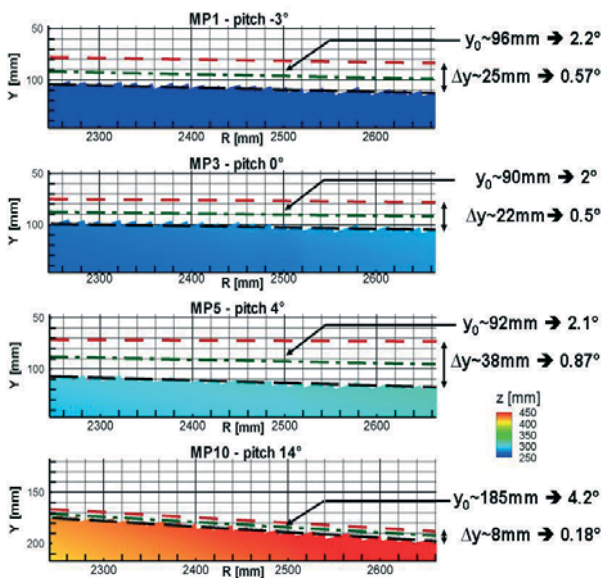


Figure 15: Lead-lag at different collective pitch angles (average and range of variation) extracted out of the IPCT-data.

The processed IPCT-data can be used to quantify the lead-lag and the magnitudes of the oscillation. Some examples are depicted in Figure 15. The four plots show the top view on the leading edge of the blade in the position of the highest lead-lag. The black dashed line identifies this highest lead-lag, while the red dashed line shows the lowest value and the green dash-dot-line gives the average lead-lag. In addition the z-value of the blade surface is colour coded to give an idea of the loading of the blade. It can be seen that for increasing angle of attack in both directions (negative and positive) the lead-lag becomes bigger. One can see that for high loading of the blade the magnitude of the oscillation becomes smaller.

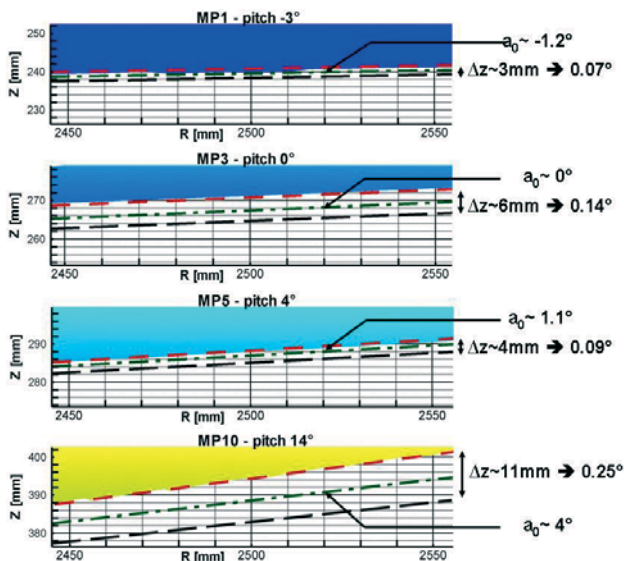


Figure 16: Coning angle and variations at different collective pitch angles extracted out of the IPCT - data and normalized to $a_0 = 0^\circ$ at pitch angle 0° .

This effect may be due to the increase of the flapping motion of the blade which is depicted in Figure 16. The four plots in this figure show the view of the blade from behind in the position of the highest position in z-direction. The red dashed line identifies this highest flapping magnitude, while the black dashed line shows the lowest value. The green dash-dot-line gives the average value of the flapping, which corresponds to the coning angle of the rotor if only collective pitch is applied. As expected, the coning angle increases for higher collective pitch angles due to the rising lift. In theory for hover state no lead-lag-oscillation and flapping motion should occur. The measured motions indicate possible subharmonic oscillations of the rotor system.

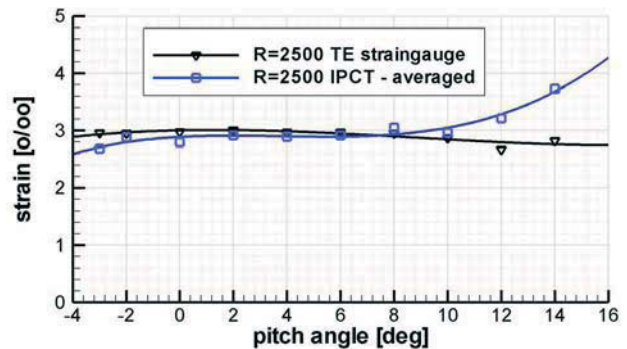


Figure 17: Strain in spanwise direction measured with strain gauges and calculated from IPCT data.

As mentioned above also strain gauges had been installed on the rotor blade at several points. Figure 17 shows the strain measured by the strain gauges at the trailing edge (TE) at the rotor radii $R = 2010$ mm and $R = 2500$ mm. In addition the strain extracted from the IPCT-data and averaged over a small area at the radius $R = 2500$ mm is depicted.

The strain in the IPCT-data was calculated by first identifying the movement of the markers then mapping the surface with the displaced markers on the reference surface and finally calculating the occurring elongation between the reference surface and the mapped surface under load.

The order of the strain magnitude of the IPCT-data is in accordance to the strain measured with the strain gauges. At higher pitch angles the IPCT-data gives higher values than the strain gauges. One reason could be the strong deflection of the rotor blade for high pitch angles and thus the decreasing viewing angle for the cameras resulting in a higher uncertainty of the method. It could also be, that the combination of the marker detection with the IPCT didn't work well with marker triples. The method relies on the boundary condition, that for the separation of the solid body movement and the local strain, the markers should not move relatively to

each other. In principle three fixed markers closed to each other (like the ones on the blade) should be enough, but the implemented software uses four markers to do the calculation with a higher certainty. Due to the fact that on the real blade only triples and not quartets are close by each other, the fourth marker was taken from the next marker triple in radial direction. This was around 600 mm away and thus a movement relatively to the other markers occurs creating the need of a tolerance in the position of the fourth marker. This tolerance has to be bigger with high angles of attack and can cause a bigger uncertainty of the method. A part of the differences may also be caused by the different reference states for both methods. For the strain gauges the blade was supported on the raised ramp of the whirl tower platform and thus straight. The reference picture for the IPCT was taken with the unsupported blade in the recording volume, because there was no possibility to place anything to hold it straight.

5. FLIGHT TEST PREPARATION

The WTT showed the abilities of the combination of QVT with IPCT for measuring the rotor blade behaviour and identified the most critical issues for the flight test planned within AIM.

The setup for the in-flight measurements needs some modification to be used on the DLR owned EC-135 FHS (Flying Helicopter Simulator), which is shown in Figure 18.

The installation of the camera system (Figure 7) and the instrumented rotor blade (Figure 8) will be the same like for the WTT. But the systems for controlling the camera system and for recording the strain gauge data have to be made by components suitable for flight testing and fitting to the FHS.

For the recording of the strain gauge data the helicopter's own data acquisition system will be used. The signals of the strain gauges will be transferred from the rotating frame to the fix frame and recorded by the acquisition system in the cargo bay.



Figure 18: EC-135 FHS.

The PC to control the camera system will be installed into a special ARINC enclosure which can be seen in Figure 19. In this figure also the display at the flight test engineer seat in the cabin is shown. On this display the camera images and the control software are visualized. The control of the software will be done with an appropriate touch pad.

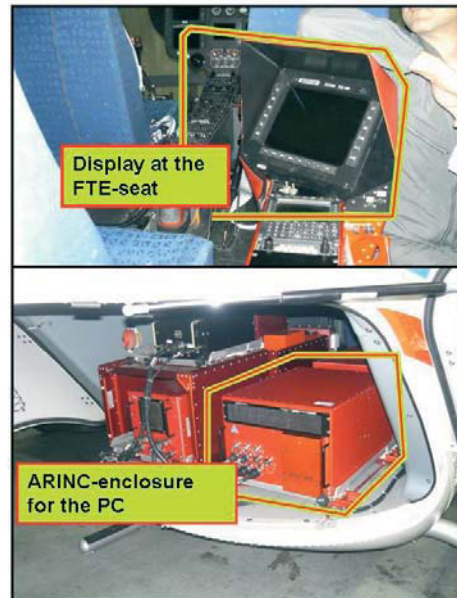


Figure 19: Installation of the measurement PC and the FTE display in the cabin.

During the creation of this paper the adaptation of the measurement PC and the certification of the camera installation and the rotor blade was in progress.

5.1. FHS Ground Test

To test the functionality of the camera setup on the helicopter in advance of the in-flight installation, a ground test (FHS-GT) with the running helicopter fixed to the ground had been performed. Figure 20 shows the setup for the FHS-GT. To check the affixing of the camera system at the EC-135 FHS, the camera support was screwed on the intended winch hard points.

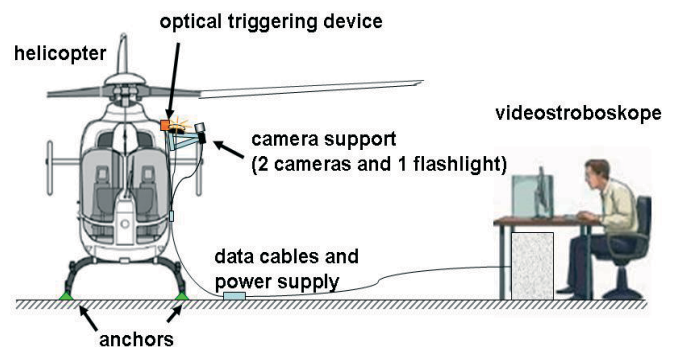


Figure 20: Setup for the FHS ground test (FHS-GT).

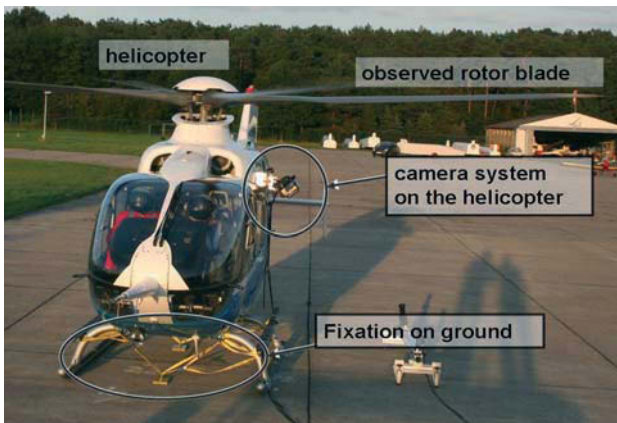


Figure 21: The running helicopter during the FHS-GT.

The High-Speed Video-Stroboscope recording system and the power supply for the strobe light had been placed beside the helicopter to have no electrical interlink between the helicopter flight control systems and the installation for IPCT. The control stand with the High-Speed Video-Stroboscope was positioned around 10 m beside the helicopter. To avoid the helicopter to take off, it was strapped to anchors in the apron using belts. The realized setup and the fixation on ground can be seen in Figure 21. The instrumented rotor blade was not available for this test but an adhesive foil with a printed dot pattern was applied to the rotor blade area under investigation to check the reachable image quality and to do a test IPCT processing of the data. During the measurement different power settings and two tilts of the rotor disc (one forward and one to the left) had been driven. An observation camera in front of the helicopter recorded the rotor disc to get an idea of the blade motion in z-direction and to verify the IPCT measurement results qualitatively.

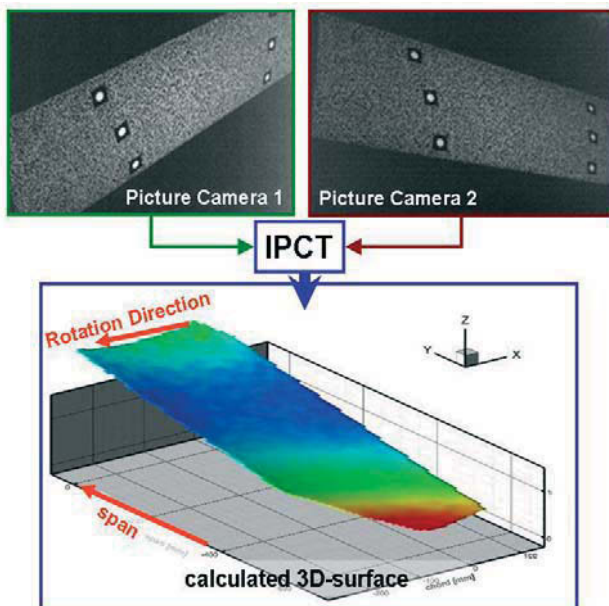


Figure 22: Camera images recorded during the FHS-GT and processed result.

5.2. Ready for take off...

The FHS-GT proved the functionality of the intended camera system on the helicopter and was also a successful fit-check for the camera support. The images recorded during the FHS-GT show sufficient quality and are processable with IPCT. In Figure 22 an image pair and one calculated 3D surface are depicted. Like in the WTT results, the shape of the blade is reconstructed very well. There is a good agreement between the horizontal movements of the IPCT-surfaces, the different measurement points and the rotor blade in the pictures of the observation camera. The change of angle of attack, that can be indicated in the IPCT results is in accordance to the steering input. Thus after finishing the modification of the PC for in-flight use and getting the permit to fly, the flight trials with the QVT-IPCT-setup can start.

6. CONCLUSION

The presented combined measurement techniques QVT and IPCT offer the advantage to measure the spatial deformation of fast moving objects in a non-intrusive way. First tests showed the applicability of the combination of the methods QVT and IPCT for measurements of the main rotor blade deformation on a flying helicopter in principle.

The camera setup is completely designed and has been tested on the helicopter during the FHS-GT successfully. Despite the rough boundary conditions for a stereo camera system on a helicopter (e.g. strong vibrations, high velocities of the observed blade) the camera setup with the High-Speed Video-Stroboscope obtained good pictures that can be processed with IPCT.

The performed WTT enabled the test engineers to verify the results achievable with IPCT against strain gauge measurements directly. The strain values obtained by the IPCT differ from the values of strain gauges but are in the right order of magnitude. The deviations may arise from the different reference positions of the blade or the change of the camera viewing angle with increasing heave of the blade. Another reason can be the use of only three markers in one chord section and an additional one in another chord section some hundred millimetres away. Solutions for this may be the application of one additional marker and the usage of the same reference state for IPCT and strain gauges.

Despite of the discovered strain differences the WTT showed the abilities of the IPCT to quantify the blade movements and the real angle of attack on the measured chords. The IPCT can thus be used as a promising tool to learn more about the blade dynamics during free flight. The measurements

within the AIM-project showed the feasibility to apply IPCT to helicopter rotors. The presented setup is able to record a cut-out of the rotor disc at one azimuth angle. In the future a setup with cameras in the rotating frame, which enables the recording of the complete rotor disc, is thinkable.

The next steps are the finalisation of the certification process to get the permit to fly and to test the method in-flight. Out of the lessons learned during the performed pre-tests, it is planned to take the reference states for the strain gauges and the cameras in the same position and at the same instant of time. If possible a fourth marker will be stucked onto the rotor blade to get a quartet of markers in the supporting chord for the strain calculations.

7. REFERENCES

- [1] Kompenhans, J. et al. (2004): *Development and application of image based measurement techniques for aerodynamic investigations in wind tunnels*. International Scientific Conference High Speed Flow Fundamental Problems, Zhukovsky, Russia
- [2] Michaelis, D.; Frahnert, H., Stasicki, B. (2004): *Accuracy of Combined 3D Surface Deformation Measurement and 3D Position Tracking in a Wind Tunnel*. ICEM12 - 12th International Conference on Experimental Mechanics, Politecnico di Bari, Italy
- [3] Kirmse, T. (2007): *Model deformation measurements in DNW-NWB within the DLR project ForMEx.*, Conference Proceedings, CD-ROM (S12-1), S. 1 - 14 ODAS 2007 8th ONERA-DLR Aerospace Symposium, Göttingen, Germany
- [4] Boden, Fritz (2007): AIM Newsletter No. 1., Newsletter (1), Göttingen, Germany
- [5] Stasicki, Boleslaw; Boden, Fritz (2008): *Application of high-speed videography for in-flight deformation measurements of aircraft propellers*, Conference Proceedings (7126-41), S. 1 - 12 28th International Congress on High-Speed Imaging and Photonics (ICHSIP 28), Canberra, Australia
- [6] Stasicki, B. (2003): *Investigation of fast, repetitive events by means of non-standard video techniques*. 7th International Symposium on Fluid Control, Measurement and Visualization (FLUCOME), Sorrento, Italy, 25-28 August 2003, paper No.231, 7 pages, CD ROM, ISBN 0-9533991-4-1
- [7] Kraus, K: *Photogrammetry. Geometry from Images and Laser Scans*. Walter DeGruyter, Berlin, 2007